To appear in:

International Journal of Nano Dimension (Int. J. Nano Dimens.)

Online ISSN: 2228-5059 Print ISSN: 2008-8868

Dates:

Received: 16 February 2026

Revised: 18 May 2026

Accepted: 13 June 2026

DOI: https://doi.org/10.57647/ijnd.2026.1704.05

Increased sensitivity in planar waveguide plasmonic nanobiosensores based on two-dimensional graphene-MoS_2 multilayers

Shabnam Andalibi Miandoab [1, *], Nazlar Ghasemzadeh [2, *], Pedram Asmand Debaglou [2]

[1] *Department of Electrical Engineering, Ta.C., Islamic Azad University, Tabriz, Iran*

[2] *Department of Biomedical Engineering, Ta.C., Islamic Azad University, Tabriz, Iran*

Corresponding Authors: sh.andalibi@iau.ac.ir , n.ghassemzadeh@iaut.ac.ir

Abstract:

This paper investigates biosensors based on plasmonic nanostructures. A plasmonic sensor using planar optical waveguide consisting of graphene and metal oxide layers has been designed and simulated for detecting biomolecules such as DNA. Plasmonics, branch of photonics, underpins many biophotonic applications, especially biosensing. Proposed biosensor relies on surface plasmon resonance in hybrid graphene/MoS_2 structure, enabling high-sensitivity detection. Sensing mechanism analyzes transmission spectrum of an electromagnetic wave launched into waveguide, which varies with refractive index changes of biomolecules near surface. Performance has been evaluated at 633 nm and for different light incidence angles. Effects of number and arrangement of graphene and MoS_2 layers on resonance angle, sensitivity, full width at half maximum (FWHM), and figure of merit (FOM) have been studied. Results show that a single graphene layer with a single MoS_2 layer yields optimal performance, with sensitivity of 193 deg/RIU and FOM of 16.6 RIU^{-1}. Minimum FWHM of 11.62° and transmission intensity T_{min} of 0.02 have been obtained. Increasing layer numbers due to optical absorption and plasmonic damping leads to higher optical losses, broader resonance curve, and reduced FOM. Electromagnetic field distribution and sensor characteristics have been analyzed via resonance angle shifts, identifying optimal structure with highest sensitivity and FOM.

Keywords: *Angle, FDTD, Graphene, Nanobiosensores, Surface Plasmon Resonance Sensitivity.*

1. Introduction

The surface plasmon resonance (SPR)-based sensors are among the most advanced label-free optical biosensors, which have great potential for application in many important fields, including medical diagnostics, environmental monitoring, and food safety, due to their high efficiency and reliability [1, 2]. Among the methods of interest to scientists to enhance sensitivity of surface plasmon resonance biosensors are use of nanoparticles and structures based on metal nanowires, as well as those based on an array of nanoholes, and usage of the hybrid nanostructures[3]. Among the advantages of this type of sensor is high sensitivity, fast response, no need for

labeling process, and timely response [4-8]. In plasmonic biosensors, there are several methods for detecting analytes, and the surface plasmon resonance method, compared to other methods, does not require a complex arrangement and provides high sensitivity. This method also has great potential for improving the integration using immobilized nanoparticles [9]. In addition, the surface plasmon resonance method also benefits from the advantages of optical transducers and is more durable and robust than other biosensors, and is also immune to other electromagnetic interferences. Surface plasmon resonance is a pioneering technique in optical sensing based on electromagnetic waves that has opened up a wide range of applications. In the last few decades, the development of SPR has been directed towards biosensing techniques. Due to the interdisciplinary nature of SPR, researchers working on concepts such as optical waveguides, thin film science, and optical detection techniques have been able to generate a great deal of practical knowledge and application in this field. SPR is also very popular due to its prevailing interdisciplinary philosophy and its simplicity of creation and use in modern research [10-14]. In SPR sensors, two main detection methods are commonly used: angle interrogation and wavelength interrogation. In the angle interrogation method, the wavelength of light is kept constant while the incidence angle is varied to measure the resonance angle shift. Due to its high sensitivity and precision, especially in monochromatic laser-based systems, this method is widely used; however, it requires accurate adjustment of the incidence angle. In contrast, in the wavelength interrogation method, the incidence angle remains fixed while changes in the resonance wavelength are measured. This method is mechanically simpler, but requires more complex spectral analysis and generally provides lower angular accuracy compared to the angle interrogation method. The surface plasmon resonance and surface plasmon waves (SPW) optical stimulation occur at the boundary between a metal and a dielectric. For this purpose, metals with negative permittivity, such as gold and silver, are used alongside dielectric materials such as liquids, gases, or solids. To stimulate surface plasmons (SPs) at a metal-dielectric boundary, free electrons in SPR-active metal must be able to resonate with incoming light at a specific wavelength. This will occur when frequency of oscillation of these surface electrons is same as frequency of light, creating resonance. Gold satisfies these criteria for SPs stimulation and has advantages such as higher practicality, the good resistance to oxidation and corrosion, the solidity, and the better function. Therefore, it is widely chosen as the acting metal for SPR [12, 15]. Since the SPR technique does not have any specific requirements, such as the fluorescence properties, the spectral signatures, or the radio signs for the molecules under study, it is frequently used in advanced bioscience laboratories. The SPR technique can even be used with colored or turbid solutions. In general, reactions of the all two-component binding that have diverse appeals in area of drug design (interactions of the protein-ligand) and membrane-associated proteins mechanisms (protein-membrane binding) and the DNA-bound proteins can be investigated through this technique. Therefore, the SPR has been successfully applied in kinetic study of ligand-receptor, antigen-antibody, and the interactions of the protein-protein. This method is also widely used in protein research and drug development. A biosensor is an analytical device designed to analyze samples of biological material to gain a better understanding of their biological composition, structure, and function, such that a biological reaction is converted into an electrical signal. Among various technologies of the sensor, structures of the optical waveguide are deemed to be invaluable tools. They suggest merits such as good control of the light path, easy measurement of light intensity of the input and output, the high sensitivity, the high degree of integration within embeddable chips, small size, the extreme resolution, indemnity to electromagnetic intervention, and potential for the distant procedure. Especially in photonic integrated circuits, the optical waveguide-based devices are more favorable

for on-chip integration than other proposed structures [16, 17]. When biosensors are used with water-based media, it is desirable for the optical waveguide sensors to work in visible wavelength ranges to compensate for the large absorption coefficient of water in the near-infrared range. The SPR technique is susceptible to changes in the refractive index in the environment surrounding the sensor. These changes occur due to the binding of the analyte (in a liquid sample) to its associated ligands (immobilized on surface of chip) when liquid instance comes into contact with surface of the sensor. So, the substance in association with liquid instance (the sensor top layer) is important in terms of index of refractive and molecules absorption [18, 19]. Two-dimensional materials are known as single-layer crystalline materials, and they are made up of a single layer of atoms. These substances are beneficial. Especially, the 2D nanomaterials such as the graphene, the hexagonal boron nitride (hBN), and the metal dichalcogenides (MX2) have allured much deliberation owing to their adequate belongings and wide applications in electronics, the optoelectronics, the energy storage facilities, the sensors, the solar cells, and the lithium batteries. Metal oxide layers refer to thin layers of semiconductor or dielectric materials composed of metal and oxygen, which are used in optical and plasmonic sensor structures. Commonly used metal oxides in SPR sensors include TiO_2, ZnO, ITO, MoO_2, and WO_2. Due to their favorable optical, electrical, and chemical properties, these materials play an important role in improving sensor performance. The use of metal oxide or semiconductor layers such as MoS_2 in SPR sensor structures enhances the electromagnetic field near the sensor surface and increases light confinement in the active region. These layers also result in a sharper resonance angle, enhanced light–matter interaction, and improved charge transfer between graphene and gold. Consequently, the sensitivity, accuracy, and overall performance quality of the sensor are significantly improved. Graphene is considered an effective material for the electronics and the optoelectronics due to its solitary composition and various essential properties, consisting the extreme carrier mobility, extreme optical clarity, adaptability, and special mechanical robustness. The studies have shown sensational potential of using the graphene for various devices of the optoelectronic, consisting the solar cells, the touch panels, the photodetectors, ultrafast lasers, polarizers, and the optical modulators. Broad absorption, the extreme carrier mobility, and short carrier lifetime make graphene a perfect material for the high-bandwidth, high-sensitivity biosensors [20, 21]. The MoS_2 covering is a barren film lubricant that operates through the sulfur atoms inherent sliding (the weak van der Waals forces). These aids decrease component have on and rectify friction coefficient. Covering is built from the extreme-purity molybdenum disulfide powder and represents special mechanical possessions, consisting extreme tensile and flexural robustness, creating it a hopeful substance for the sensors, the transistors, and flexible electronic devices. MoS_2 has arisen as a hopeful substance for electronic applications owing to its high electron mobility. This material has unique optical properties that make it an appealing substance for the development of optoelectronic devices such as the photodetectors, the solar cells, and the light-emitting diodes. It has also been widely used in electrochemical biosensors due to its good conductivity, the fast charge transfer rate, and outstanding electrocatalytic activity. MoS_2 nanostructures are an alternative to toxic heavy metals, exhibiting biocompatibility, low toxicity, and high stability and affinity for biomolecules. The electrochemical range of MoS_2 is from -0.6 V to +0.7 V. Such a limited working potential, which is the characteristic of it, prevents detection of essential analytes such as the nitroaromatic volatile, pesticides, and mycotoxins, which are alternatively observable on carbon surfaces.

Bibikova *et al.*, (2017), studied the plasmonic chip-based systems consisting of the gold nanostars assembled on silicon substrates. In which, extreme aspect ratio gold nanostars structure provides a larger number of hot spots on their surface, leads to an enhancement of the electric field around

nanomaterials[22]. Salazar *et al.*, (2018), reviewed new trends in plasmonic sensing. In plasmonic sensing, they focused on improving the performance of SPR sensors using magnetic nanoparticles and metamaterials, as well as developing uniform, flexible, and reproducible surface-enhanced Raman scattering (SERS) substrates [23]. Lai *et al*., (2018), proposed a plasmonic filter and sensor based on a hexagonal resonator coupled to metal–insulator–metal (MIM) waveguides. They demonstrated that by using metallic blocks inside the resonator, multiple transmission peaks as well as asymmetric Fano resonances could be generated. The FDTD simulation results indicated high refractive index sensitivity and a high figure of merit for the proposed structure, making it suitable for integrated photonic applications and on-chip optical sensors [24]. Li *et al.,* (2019), designed a hybrid plasmonic-metal graphene sensor for multispectral sensing in near and mid-infrared regions, which simultaneously performed multispectral sensing in near and mid-infrared areas[25]. Tsuchikawa (2020), investigated the effect of surface-enhanced infrared absorption (SEIRA) and dispersion-based SPR for the detection of 2,4-dinitrotoluene (2,4-DNT). By placing 2,4-DNT on metal-insulator-metal (MIM) resonator arrays, they observed that the natural dispersion of the mixed refractive index combined the effect of SEIRA and SPR[26]. Ebadi *et al.*, (2020), designed and numerically investigated a highly compact plasmonic filter based on metal–insulator–metal (MIM) waveguides. In this structure, Fabry–Perot cavities were used to create tunable multiband filters in telecommunication wavelengths. Their results showed that the proposed structure can achieve band-pass filters, cutoff filters, and plasmonic absorbers with extremely small dimensions, making it applicable to integrated photonic circuits and optical communication systems [27]. Wen *et al*., (2021), proposed a graphene-based plasmonic system for advanced molecular infrared spectroscopy. The system consists of two graphene layers separated by a nanometer gap. This structure can support acoustic graphene plasmons (AGP), which leads to super-concentration of the electromagnetic field and substantial field enhancement inside the nanometer gap [28]. Patel *et al*., (2021), reviewed research results on a tunable infrared biosensor for detecting hemoglobin in the range of 1.5 to 165 μm. This biosensor is made of phase change materials that change their phase with temperature, providing tunability of the sensor. This feature enables selective detection of hemoglobin [29]. Bensalah *et al.,* (2023), designed a high-sensitivity plasmonic sensor based on a metal–insulator–metal (MIM) waveguide structure and a hexagonal ring resonator using the FDTD method. Their results demonstrated a linear relationship between the refractive index of the medium and the resonance wavelength shift. The proposed structure achieved a maximum sensitivity of 2417 nm/RIU and a figure of merit of 38, and in addition to biomolecule detection, it was also applied for temperature sensing [30]. Faraji *et al*., (2025), proposed a novel plasmonic biosensor based on 3D cylindrical hyperbolic metamaterial nanolenses in 2025. Their results showed that the proposed biosensor has the potential for high-sensitivity, selective detection of biomolecules[6]. Miandoab and Hars (2025), investigated a focused plasmonic nanostructure optical antenna at visible wavelengths. They studied the effects of shape and size of plasmonic nanostructure to increase the gain and improve the focusing of the optical antenna relative to the small detector area[31]. Skakya *et al*. (2026), presented a comprehensive review of the evolution of smart sensors based on photonic crystal fibers and surface plasmon resonance (PCF-SPR). They investigated the applications of these sensors in the biomedical field, including the detection of disease biomarkers, DNA, proteins, glucose, and pathogenic microorganisms, and demonstrated that due to their very high sensitivity, real-time monitoring capability, miniaturization, and multiplex detection, these sensors are highly suitable for next-generation diagnostic systems. The researchers also discussed future challenges and opportunities, including the use of artificial intelligence and hybrid models to optimize sensor performance [32]. Ramola *et al*. (2026), designed

a photonic crystal fiber- and SPR-based biosensor for the early detection of cancer cells. Using FEM simulations in COMSOL, they demonstrated that a quasi-D-shaped structure combined with PMMA and gold layers exhibits very high sensitivity in detecting refractive index changes of cancer cells [33]. Ramola *et al.* (2025), designed an SPR sensor based on a Kagome structure in a photonic crystal fiber to detect blood components and biomarkers with high sensitivity. They evaluated the sensor performance for different materials such as glucose, hemoglobin, and BSA and achieved very high sensitivity and resolution [34]. Ramola *et al.* (2025), published a comprehensive review on recent advances in photonic crystal fiber-based SPR sensors. They compared different designs, plasmonic materials, and biosensing applications, and investigated the role of these sensors in detecting diseases, DNA, glucose, and cancer cells [35]. Ramola *et al.* (2025), designed a novel SPR sensor with a square structure and an Au–TiO_2 interface. In addition to FEM modeling, they investigated the role of artificial intelligence and machine learning in optimizing the performance of photonic sensors and demonstrated that AI can improve the accuracy and adaptability of these sensors [36]. Ramola *et al.* (2025), investigated different optical biosensor technologies for early cancer detection. They compared the performance of SPR, LSPR, Raman, fluorescence, and optical fiber sensors and explained the advantages and applications of each in cancer diagnosis [37]. Skakya *et al.* (2023), designed a low-cost spectroscopy system to investigate the optical properties of different edible oils. They analyzed four samples, including olive oil, mustard oil, amla oil, and red palm oil, in terms of transmission and absorbance. The results showed that each oil exhibits different spectral behavior at different wavelengths, and these differences can be identified using linear relations and mathematical modeling [38]. Studies show that penetration depth plays an important role in determining the interaction strength between the plasmonic field and the sensing environment, and consequently the performance of SPR sensors. It has also been reported that penetration depth depends on parameters such as metal layer thickness, stimulation wavelength, multilayer structure, and the optical properties of two-dimensional materials. In addition, the use of two-dimensional materials such as graphene and MoS_2 can improve field confinement, increase electromagnetic field localization, and enhance plasmonic coupling, ultimately leading to improved sensitivity and biosensor performance. Some studies have also shown that changing the number of layers and hybrid plasmonic structures can modify the evanescent field distribution and its penetration depth, thereby directly affecting the interaction between the field and the analyte. Furthermore, optimization of penetration depth has been introduced as one of the key factors in improving detection efficiency and enhancing the biosensing response of SPR sensors, and it plays an important role in the design of plasmonic structures based on two-dimensional materials [39-46]. Graphene and the graphene oxide supply acceptable aid for the adsorption of biomolecules owing to their enormous surface area and π affluent conjugated system structure, creating them appropriate dielectric layers for SPR sensing. Nevertheless, graphene generates greater attenuation in surface plasmons owing to the enormous imaginary dielectric capacity of the upper layers of the graphene, thereby reducing the detection precision. In the case of high function in the SPR biosensors, devices based on hybrid substances that include graphene and photosensitive substances can be very effective. This hybrid material system can exploit extreme carrier mobility properties of the graphene and powerful coefficient of absorption of photosensitive materials, and so concurrently maximize both aspects of harvesting of light and light-induced carrier ancestry[47-53], To take advantage of the above, in this paper, we have evaluated and studied the performance of the proposed optical biosensors for detecting DNA hybridization using the angular modulation method. This method offers excellent sensitivity to refractive index alternations in case of a planar optical waveguide-based SPR biosensor. To achieve this goal, by accurately introducing the structures and examining the characteristic spectrum of light passing through the waveguide in

response to changes in the angle of the incoming light, we have tried to introduce an optical biosensor with appropriate sensitivity and detection resolution through design and simulation. The main novelty of this paper compared to the study by Rahman *et al.* (2017), have been performed in both the proposed structure and the type of physical analysis. While the previous study mainly investigated a limited hybrid structure based on MoS_2 and graphene for DNA hybridization detection, in this paper several different arrangements of graphene and MoS_2 layers, including single-layer, multilayer, and asymmetric hybrid structures, have been comparatively analyzed. In addition, the effect of increasing the number of graphene/ MoS_2 layer pairs has been investigated. This comparative analysis enables a detailed study of the effects of layer number and arrangement on resonance angle, sensitivity, FWHM, and figure of merit (FOM). Furthermore, unlike previous studies, this paper provides a more detailed physical analysis based on electromagnetic field distribution, plasmonic confinement behavior, evanescent field penetration depth, and optical losses. The results show that the structure containing one graphene layer and one MoS_2 layer provides stronger field confinement near the sensor surface and enhances the interaction between light and biomolecules. This leads to a larger resonance angle shift and improved sensor sensitivity. The analyses also demonstrate that increasing the number of graphene and MoS_2 layers increases optical absorption losses and plasmon damping. This results in broadening of the resonance curve, increased FWHM, reduced field penetration depth, and ultimately lower sensitivity and detection precision. In addition, the proposed planar waveguide structure offers simpler fabrication and better integration capability compared to many fiber-based structures. The optimized structure introduced in this paper has achieved a sensitivity of 193 deg/RIU and a figure of merit of 16.6 RIU^{-1}, confirming the high performance of the proposed structure.

2. Materials and Methods

2.1. Optical Waveguide-Based Biosensor Structure

The proposed design consists of a flat waveguide located in the y-z plane to guide single-mode input and output light without loss. This sensor region uses an extreme layer of the refractive index sandwiched between two lesser layers of the refractive index to trap light and guide it to the output. At one section of the length of the waveguide, multilayer metal of (Au)-graphene-photosensitive layer (MoS_2) of sensor is located, which acts as the interface section with the detection sample. The front view of the cross-sectional considered sensor of SPR based on 2D material plasmonic waves has been shown in Fig. 1. The layer arrangement has been considered as waveguide / Au / MoS_2 / graphene / analyte, such that the graphene layer is directly in contact with the sensing environment. The reason for selecting graphene as the top layer is its high surface area, suitable biocompatibility, and its ability to effectively adsorb biomolecules, which enhances the interaction between the evanescent field and biological molecules. Key limitations for designing an SPR sensor include the appropriate selection of materials for the different layers, the choice of the metal material to form the sensor surface and the operating wavelength, and the appropriate selection of the number and dimensions of layers to create waveguides and create plasmon resonance parameters to increase detection efficiency. The usage of a substrate glass with a low refractive index provides easier phase matching among the waveguide and surface plasmon modes in a device when acting in an aqueous environment (n = 1.33).

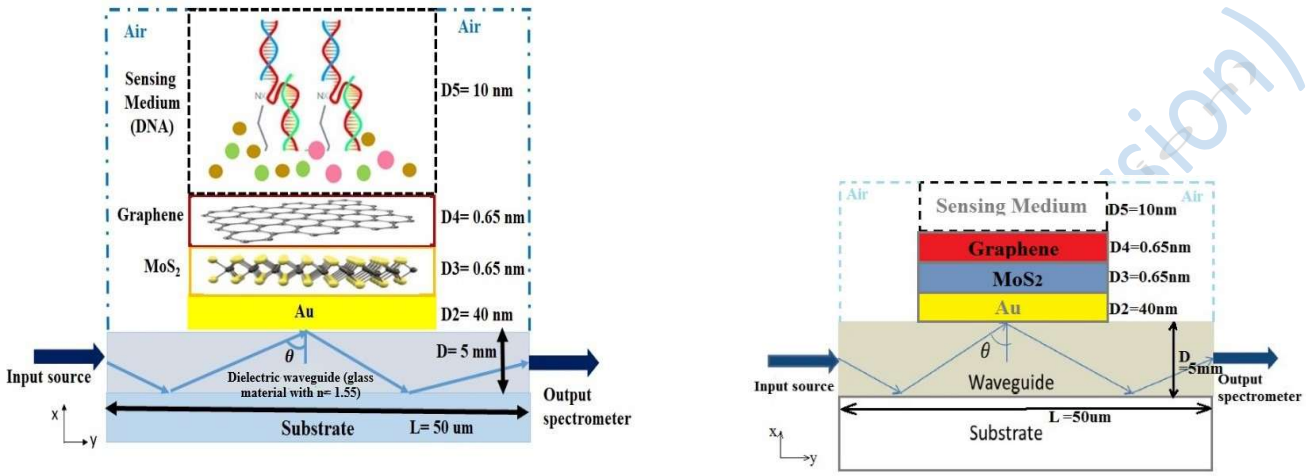

Figure 1. Layer-by-layer structure of the optical waveguide biosensor as seen from the front.

The substrate glass with a refractive index of 1.46 has been chosen to make the process of creating a waveguide easier and more cost-effective. The PW SPR sensor has been intended for using in aqueous solution based

a) b)

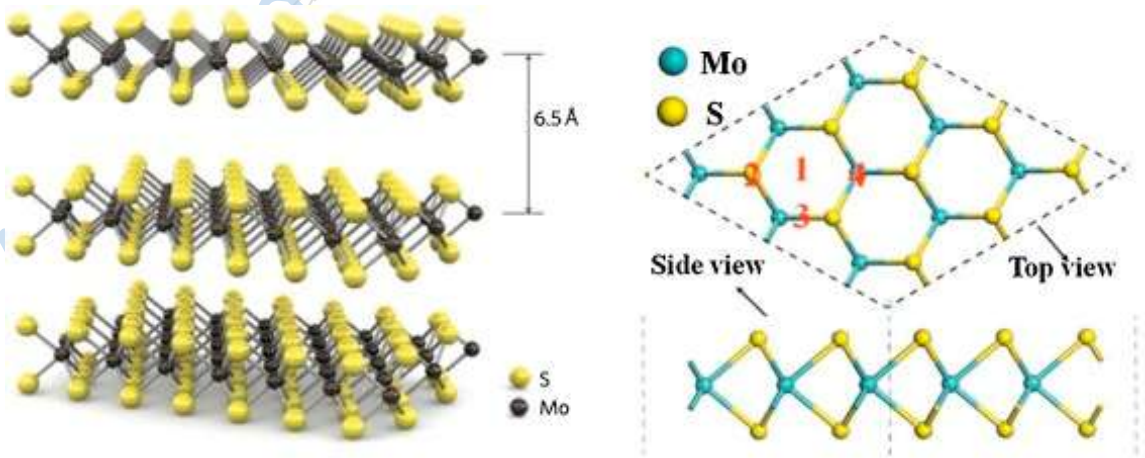

Figure 2. a) Crystal structure of MoS_2 molecules, b) Top view and side views of the MoS_2 structure.

on solidity and inertness of metal film to outer surrounding. Sensor performance is reduced by changing optical possessions of film. Gold is often chosen for these structures because it is chemically inert and adheres well to glass substrates. Besides, the gold films supply outstanding electrodes for the electrochemical studies. In our desired biosensor, a coating of a graphene- MoS_2-hybrid structure has been used in addition to gold. Due to the high adsorption capacity, high mobility of the graphene carriers, and powerful coefficient of the absorption of photosensitive substances, this hybrid system can simultaneously maximize both aspects of light collection and light-induced carrier extraction, ultimately improving detection sensitivity. Also, in our studies, water environment has been considered as a comparative reference sensing environment. The proposed structure has been selected due to the simultaneous combination of the plasmonic properties of metals, the high electronic conductivity of graphene, and the strong optical properties of MoS_2. This combination enhances electromagnetic field confinement and improves the interaction between light and biomolecules. Unlike many previous structures that employed only metals or a single two-dimensional material, this study systematically investigates the effect of the combination and number of graphene/ MoS_2 layer pairs. The results demonstrate that the proposed structure provides higher sensitivity, smaller FWHM, and better integration capability compared to many conventional structures. The two-dimensional simulation was selected due to the longitudinal symmetry of the structure and the uniform geometry along the propagation direction. In such structures, the main plasmonic behavior and electromagnetic field distribution can be effectively modeled in a two-dimensional plane. The use of a two-dimensional model significantly reduces computational time and memory requirements while accurately preserving the main SPR characteristics, resonance angle, and field behavior. Therefore, two-dimensional simulation in this study represents a valid and commonly used simplification for the preliminary analysis of planar waveguide structures. In the fabrication of layered structures such as Au / MoS_2 / graphene, dry transfer and deterministic layer-by-layer stacking methods are commonly used to preserve the precise layer sequence while minimizing contamination and tearing. In this approach, each two-dimensional layer is individually picked up using a soft polymer stamp such as PDMS or PPC and then accurately placed on the previous layer under microscopic alignment. Since this process is performed without chemical solutions, polymer residues and contamination are minimized. In addition, to prevent tearing, the peeling speed is reduced and soft substrates are used to decrease mechanical stress. In more advanced methods such as pick-up transfer, a carrier layer (such as PPC) first picks up the graphene layer, and then the remaining layers are sequentially collected to form a clean and well-controlled stack. These methods have been widely used for fabricating graphene/ MoS_2 heterostructures and even interfaces with metals such as Au, and have been confirmed in the literature as standard approaches for producing clean interfaces [54-57]. Although this work is simulation-based and its main focus is not on fabrication processes, the fabrication of layered structures such as Au/ MoS_2/graphene is experimentally feasible. Various studies have shown that such heterostructures are commonly fabricated using dry transfer methods and van der Waals assembly techniques. In these methods, polymer stamps such as PDMS or PPC are used for sequential pickup and placement of two-dimensional layers, allowing precise control over the layer order while avoiding contact with chemical solutions. This significantly reduces interface contamination and improves interface quality. However, challenges such as residual polymer contamination, mechanical strain during transfer, and difficulties in achieving atomically clean interfaces between metals such as Au and two-dimensional semiconductors such as MoS_2 still remain. In addition, maintaining large-scale uniformity and preventing tearing during layer transfer are among the experimental limitations of these methods. Despite these challenges, experimental

studies have demonstrated that deterministic stacking and dry transfer techniques enable the fabrication of such structures with high precision [54-57].

A six-layer sensing structure is investigated using the FDTD method, considering the optical and electrical properties of each layer. The structure consists of a waveguide with thickness D, coated with a gold film of thickness D2, an MoS_2 layer with thickness D3, and a graphene monolayer with thickness D4, followed by a biomolecular detection medium. The crystal structure of MoS_2 is composed of a hexagonal plane of Mo atoms located between two hexagonal planes of S atoms. Strong covalent bonds exist between Mo and S atoms, while adjacent layers are connected through weak van der Waals forces. The molecular structure of MoS_2 is illustrated in Fig. 2, where the crystal structure is shown in Fig. 2a, and the top and side views are presented in Fig. 2b. In the proposed model, the first layer is the waveguide and the second layer are the metal layer, whose complex dielectric function is described using the Lorentz–Drude model. The refractive indices of the two-dimensional MoS_2 and graphene layers are considered as $n_3 = 5.9 + 0.08i$ and $n_4 = 3 + 1.1487i$, respectively [57]. The refractive index values of MoS_2 and graphene at the wavelength of 633 nm differ across various studies because the optical properties of two-dimensional materials depend on factors such as the number of layers, fabrication method, crystalline quality, growth conditions, and the optical model used. In this study, the values of $n = 5.9 + 0.08i$ for MoS_2 and $n = 3 + 1.1487i$ for graphene were selected based on the values reported in studies related to SPR sensors and plasmonic structures in the visible region [58]. The main objective of this research was to investigate the relative behavior of the hybrid structure and compare the performance of different layer configurations.

Fourth layer is sensing medium and its refractive index is $n_s = 1.33$ as a reference for comparison with the aqueous medium. The DNA hybridization measures degree of genetic relation among sets of the DNA sequences to determine genetic gap between two organisms. The sensing DNA hybridization is essential for obtaining information about the DNA molecular linkage, through many human diseases can be directly diagnosed. In this case, refractive index for sensing medium changes owing to DNA immersion in sensing medium. altered refractive index of the sensing medium (n_s^a) after the absorption of the DNA molecules is considered by equation 1 [58]:

$$n_s^a = n_s + c_a \frac{dn}{dc} \quad (1)$$

c_a is adsorbed molecules concentration (1000nM), n_s is refractive index of sensing medium before adsorption of the DNA molecules, and dn/dc is refractive index increase owing to adsorption. If a standard buffer solution is used, refractive index increase parameter is taken as $dn/dc = 0.182$ cm^3/gm^2. With this relation, sensing medium refractive index being detected increases from 1.33. To study these changes, refractive index of medium is considered to vary from 1.33 to 1.39.

2.2. Applying the Finite Difference Time Domain (FDTD) Method to the SPR Sensor

The method of finite difference time domain is a computational method that directly solves time-dependent Maxwell equations using the exact second-order central difference in time and space, and considers both electric and magnetic fields. Finite difference time domain method has been significantly improved to the point where it is used in various applications including nano-optics and nano-photonics. FDTD is a numerical method used to solve Maxwell's equations for the

distribution of electric and magnetic fields in both the time and space domains. Basis of this method is the gridding of the space under study into small elements and Yee algorithm is typically used to solve electromagnetic problems.

The FDTD method solves Maxwell's differential equations using the central finite difference technique in both time and frequency domains. Since conventional approximations become inaccurate at nanometer scales comparable to optical wavelengths, FDTD is widely used for electromagnetic analysis of nanoscale structures. In this method, the simulation space is divided into small cubic cells containing electric and magnetic field components. Finite difference equations are then used to update the field values over time based on neighboring cells and previous time steps. After the simulation is completed, the electromagnetic field distributions are used to calculate the desired physical properties.

In numerical methods such as FDTD, a fictitious absorbing boundary condition named a perfectly matched layer (PML) is used to simulate problems with open boundaries in order to shorten the computational space. Also, by using this layer, the reflection of electromagnetic waves into the structure from the computational spatial edges in the FDTD method used for a structure with a non-uniform grid has been used. The 3D inhomogeneous network with one-dimensional coordinate grid nodes is as follows: $\{y_j, j = 1, N_y\}$; $\{z_k, k = 1, N_z\}$.

2.3. S Sensitivity characteristic and characteristic of the Factor of Merit (FOM)

Sensitivity of a sensor of SPR shows rate of alternation of the SPR resonance angle in response to alternations in refractive index of sample medium (material under test). In other words, the sensitivity expresses how sensitive the sensor is to minor alternations in refractive index of medium and is defined by equation 2 [58,59]:

$$S = \frac{d\theta_{SPR}}{dn} = \frac{\Delta\theta_{min}}{\Delta n_s} \qquad (2)$$

S is the sensitivity of the sensor, $d\theta_{SPR}$ is alternation in resonance angle, and dn is alternation in refractive index of the sample medium. Larger value of S, more sensitive the sensor. This means that small changes in the refractive index of the sample medium produce larger changes in the resonance angle, making these changes easier to detect. High sensitivity is crucial for accurate and early detection of changes in biological or chemical samples.

The factor of merit is a unique criterion for comparing the performance of different sensors and a general criterion for evaluating the performance of a sensor that takes into account sensitivity and precision together. A sensor with a higher FOM generally performs better. Sensitivity (S) indicates how sensitive the sensor is to changes in the refractive index. FOM is defined as the sensor sensitivity divided by the bandwidth of the surface plasmon resonance curve (FWHM), and is calculated by equation 3 [58, 59].

$$\text{FOM} = Q_f = \frac{\text{S}}{\text{FWHM}} \quad (3)$$

FOM is figure of merit, S is sensor sensitivity, and the FWHM is full width at half maximum of surface plasmon resonance curve. High sensitivity (large S) increases the FOM. Low bandwidth (small FWHM) also increases the FOM. A low bandwidth indicates a higher precision in determining the resonance angle. Therefore, a sensor with a high FOM has both good sensitivity and high precision in detecting the resonance angle.

2.4. Simulated structure of the desired optical biosensor

In this section of the paper, we have considered the simulated structure of the optical biosensor under study in two dimensions and the arrangement of the layers including MoS_2 and graphene in the front view, which has been implemented in the Lumerical software environment, and shown in Fig. 3. The Lumerical software package has been used for the simulation, which uses the FDTD Solutions method in 2D to perform optical response calculations and electric field distribution on the designed structure. The radiation field distribution is emitted as a light source with a wavelength of 633 nm from a monochromatic laser source (a red visible light source) and the data is gathered employing a spectrometer and computer numerical calculations. In this study, the wavelength of 633 nm was selected due to its widespread use in SPR sensors, the availability of optical data for materials, and the possibility of direct comparison with previous studies. Since the wavelength of 633 nm is compatible with common He–Ne lasers and visible light sources, and is one of the most widely used wavelengths in laboratory SPR and biosensing systems, this wavelength has been also investigated in the present study. For focusing structure with same periodicity, source is assumed as a plane wave. For this purpose, we have assumed propagation direction to be perpendicular to structure surface (x-axis positive direction) and accomplished calculations on structure surface, in x-y plane. We have performed calculations on structure surface, in x-y plane. For simulation, only a 250nm periodicity period is modeled and the boundaries created in y direction are periodic boundary conditions. In x direction, where structure is not periodic, boundary conditions of PML have been assumed. To ensure extreme precision of calculations in proportion to structure used, of mesh cells size used for specified simulation area has been assumed to be about 0.2nm. To ensure that the results are independent of the mesh size, a convergence test was performed. The results obtained from several different mesh sizes were compared, and it was observed that for meshes smaller than the selected value, no significant changes occurred in the resonance angle or transmission spectrum. Therefore, the selected mesh size guarantees appropriate accuracy and numerical stability of the results. The simulations were carried out using the Finite-Difference Time-Domain (FDTD) numerical method, which is one of the standard approaches for analyzing plasmonic structures and investigating electromagnetic field distributions. To ensure result accuracy, a very fine mesh was employed in sensitive regions such as the metal–dielectric interface and the two-dimensional layers. The mesh size in these regions has been considered to be approximately 0.2 nm, while larger mesh sizes have been used in other regions to reduce computational cost. In addition, a convergence test was performed to verify the independence of the results from the mesh size, and it was observed that with further reduction of the mesh size. there is no significant change in the resonance angle and transmission spectrum. Therefore, the selected mesh size provides a suitable balance between accuracy and computational cost. To realize this biosensor, a planar waveguide has been shaped of a dielectric core, which is

located between two cladding layers with a lower refractive index. In both cases, the propagation and guidance of light along the core will occur based on the well-known phenomenon of total internal reflection. The angle of incidence of light into the waveguide is swept between 50 and 90 degrees and the amount of transmitted and reflected light in the sensing region has been calculated. We have shown how angle of resonance changes with varying refractive index. The proposed structure is based on a planar optical waveguide in which the input light propagates through the waveguide core and interacts with the Au metal layer and the two-dimensional layers in the sensing region via the evanescent field. In the FDTD model, this mechanism was simulated using a TM-polarized light source with propagation along the waveguide direction in order to accurately model surface plasmon resonance excitation at the metal–dielectric interface. It was also clarified that the angular sweep in the simulation has been performed only to extract the resonance conditions and determine the

SPR angle, and does not imply direct free-space illumination of the structure. In practice, the light is first guided inside the waveguide and then plasmonic coupling is generated at the Au/ MoS_2/graphene interface. In Fig. 3, the light propagation direction (y), plasmonic coupling direction toward the sensing region (x), source position, sensing region, PML boundaries, and the location of surface plasmon resonance formation are clearly illustrated to ensure complete consistency between the schematic structure and the simulation model.

The simulations were carried out using the Lumerical FDTD Solutions software package. The computational platform consisted of a workstation equipped with a multi-core Intel Core i7 processor, 32 GB of RAM, and a 64-bit operating system. To reduce computation time, parallel CPU processing was enabled, allowing the FDTD calculations to be distributed across multiple cores. In some cases, GPU acceleration was also utilized for computationally intensive tasks when available. To improve accuracy while minimizing computational cost, Adaptive Mesh Refinement (AMR) was employed. This approach enabled high-resolution meshing in critical regions of the structure, thereby preventing errors caused by insufficient sampling of the electromagnetic fields. The mesh size was adjusted intelligently to maintain accuracy while optimizing memory consumption. This combination of hardware resources and optimization techniques provided accurate simulations within reasonable computational time and resource usage. The angle sweep in the simulation has been performed solely to determine the resonance conditions and analyze the SPR response, and does not necessarily imply direct injection of light into a real waveguide at very large angles. In practical structures, one of the most common and applicable methods for coupling light into a waveguide is the use of prism coupling or grating coupling, which enables precise adjustment of the angle and phase matching between the waveguide mode and the surface plasmon mode. In these methods, the effective propagation angle is controlled through the coupling conditions, and there is no need for direct free-space injection of light into the waveguide at extremely large angles. In addition, the use of rotational stages and optical alignment in SPR setups allows precise and continuous adjustment of the coupling angle. Therefore, the investigated angular range in the simulations has been considered for extracting resonance conditions and studying the sensor behavior.

3. Results and discussions

In this section, to investigate and analyze biosensors based on plasmonic nanostructures of 2D materials, first the structure of the biosensor based on the optical waveguide and the simulated structure of the desired biosensor in this study have been introduced. Then, the results of the field distribution and power spectrum transmitted through the waveguide sensor with different layers of MoS_2 and graphene have been analyzed and investigated. Since SPR sensors are one of the most effective and advanced optical biosensors with the highest efficiency in the field of medical diagnosis, to design and enhance sensitivity of this type of the biosensor, nanoparticles and the structures based on metal nanowires, an array of nanopores, and hybrid nanostructures have been used.

According to the structure considered in Fig. 1, the biosensor has been studied from a front view. A waveguide layer as the waveguide core (Dielectric waveguide glass material with refractive index of 1.55) with a higher refractive index n_c=1.55 is placed between two substrate layers with a refractive index n_s=1.46 and air with a refractive index of one. Owing to high refractive index of the core compared to the top and bottom sides, the light entering it is confined and guided to the end at the waveguide surface. The waveguide has a length of 50 micrometers, and sensing conditions have been provided in its middle region. The waveguide layer has a diameter of 5 mm and is covered with a 40 nm thick gold layer. Since the proposed structure is modeled based on a planar waveguide with dimensions larger than those of conventional integrated photonic waveguides in order to provide stable wave propagation and proper coupling of the evanescent field with the plasmonic layers and two-dimensional materials, a waveguide diameter of 5 mm has been considered. In this model, the main purpose is not to design a compact photonic or single-mode waveguide at the micrometer scale, but rather to investigate SPR behavior, resonance angle variations, and the effect of graphene/ MoS_2 layers on sensor performance. Therefore, the use of larger waveguide dimensions leads to improved FDTD simulation stability, reduced numerical boundary effects, and more accurate analysis of the plasmonic response of the structure. In addition, since the plasmonic field is mainly concentrated in the metal surface and sensing layer regions, the overall dimensions of the waveguide do not have a dominant effect on the main SPR mechanism in the proposed structure.

The value of 0.65 nm for the graphene layer thickness in this study has been selected as an effective optical thickness in the FDTD simulation and does not merely represent the ideal physical thickness of monolayer graphene. Although the structural thickness of single-layer graphene is commonly reported to be around 0.34–0.35 nm, larger values are often used in electromagnetic models and optical simulations to more accurately represent the optical response of graphene. In FDTD simulations, graphene is modeled as a layer with an effective complex refractive index, and therefore its effective optical thickness may differ from its actual physical thickness. Selecting a value of 0.65 nm improves numerical stability, allows more appropriate mesh definition, and provides more accurate modeling of the interaction between the electromagnetic field and the graphene layer. In addition, similar values have been used in some previous studies [58,60] on graphene-based SPR sensors. Since the main objective of this study was to investigate the relative behavior of the structure and the effect of graphene/ MoS_2 layers on the plasmonic response of the sensor, the use of the effective thickness value of 0.65 nm does not significantly affect the overall trend of the results or the main SPR mechanism.

The thickness of 40 nm for the Au layer has been selected based on previous studies related to waveguide-based SPR structures and hybrid plasmonic structures, since this thickness can provide an appropriate balance between surface plasmon resonance excitation and reduction of optical

losses. Although a thickness of around 50 nm is commonly used in many Kretschmann structures, the coupling conditions in the present waveguide-based structure are different [58,59]. In this structure, the thickness of 40 nm resulted in an appropriate resonance dip and effective coupling of the evanescent field with the MoS_2 and graphene layers. In this study, the primary focus was on investigating the effect of two-dimensional layers. A 0.65 nm thick MoS_2 photosensitive monolayer is formed on the gold. Finally, a 0.65 nm thick graphene monolayer is placed on the sensor adjacent to the sensor detection layer. A 10 nm thick sensing detection area is considered on graphene. In the initial conditions without biomolecules, this environment is aqueous and its refractive index is 1.33.

In this study, the sensing region with a thickness of 10 nm has been considered as an effective sensing region for modeling the interaction between the evanescent field and DNA molecules. In practice, DNA molecules after immobilization on the sensor surface are not arranged as a perfectly compact and ideal layer; rather, the spatial structure, molecular orientation, inter-strand spacing, linker layers, and surrounding environment can create an effective optical region larger than the actual physical thickness of DNA. Although the physical thickness of DNA is usually reported within a few nanometers, in many SPR models a larger effective sensing layer is considered in order to account for the complete interaction between the evanescent field and biomolecules. Since the evanescent field decays exponentially away from the sensor surface, the sensor sensitivity depends on the thickness of the sensing region, and increasing the thickness of the effective analyte layer can alter the overlap between the field and biomolecules. In this study, the value of 10 nm has been selected as the minimum effective analyte region on the sensor surface for modeling the optical response of DNA hybridization. The main purpose of this research is not to precisely model the physical thickness of a specific DNA sequence, but rather to investigate the relative behavior of the sensor against refractive index variations.

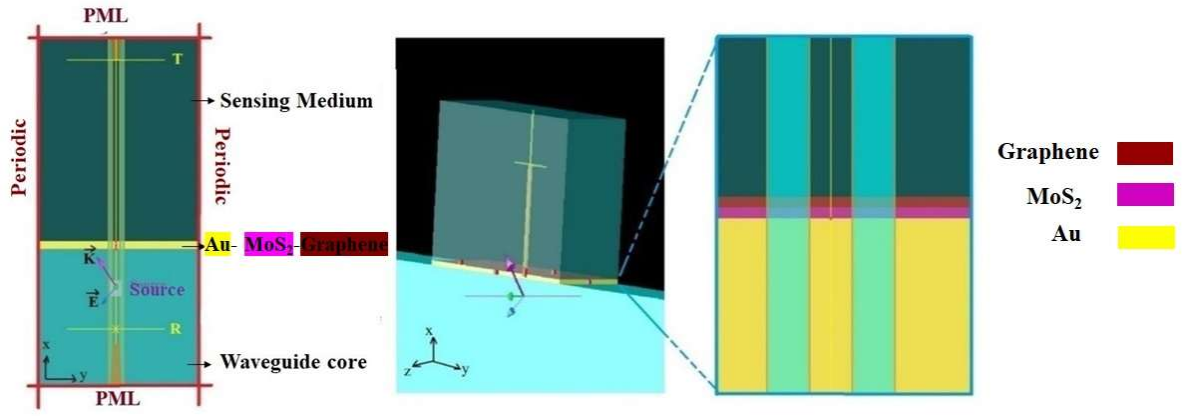

Figure 3. The designed structure in the simulation environment of the desired optical biosensor.

3.1. Field distribution and power spectrum transmitted through a waveguide sensor with different structures of MoS_2 / graphene bilayer

To demonstrate performance of the desired biosensor similar to the structure considered in Fig. 1, the angle modulation method has been used. For this purpose, laser light at 633nm is radiated into the waveguide region. The electromagnetic field distribution is calculated by the FDTD numerical

solution method in different regions of the structure. It is obtained proportional to the distribution of the light field passing through the waveguide after reflection from the created sensing area. Changing light incidence angle according to sensing area refractive index creates different reflected light power, which is plotted as a variable with the angle of light entry at a specific angle to obtain a minimum value for the light power passing through the waveguide. The minimum angle value alters with alternation of sensing medium, which forms basis for calculating the sensitivity in this type of biosensor. In Fig. 4a, the distribution of the electric field with respect to different layers with changing angles, and in Fig.4b, the power transmission curve with respect to angular changes for sensing media with different refractive indices have been depicted. The electromagnetic field distribution results show that the stronger the field confinement near the sensor surface, the greater the interaction between light and biological molecules, enabling more accurate detection of very small refractive index changes. This strong field confinement increases the SPR resonance angle shift, improves sensitivity, and lowers the sensor detection limit. In the hybrid graphene/ MoS_2 structure, due to the stronger confinement of the electromagnetic field in the sensing interface region, the sensor performance is significantly improved and higher sensitivity is achieved. To investigate plasmonic field coupling and penetration depth behavior, the electric field distribution in Fig. 4a and Fig. 6a was analyzed in greater detail. As observed in these figures, the electromagnetic field is strongly concentrated at the Au–dielectric interface, indicating successful excitation of surface plasmon resonance. It is also shown that although the evanescent field decays exponentially inside the Au layer, part of the field still penetrates through the metal layer into the MoS_2, graphene, and sensing regions. This confirms that the two-dimensional layers placed on Au are located within the effective sensing region and can interact with refractive index variations in the surrounding environment. In addition, the penetration depth in Au-based SPR structures at the wavelength of 633 nm is typically reported to be within the range of several tens of nanometers. Despite the 40 nm thickness of the Au layer, the strong field localization at the metal–dielectric interface and the coupling established in the proposed hybrid structure preserve effective interaction between the field and the MoS_2/graphene layers. For greater clarity, the layer boundaries and sensing region

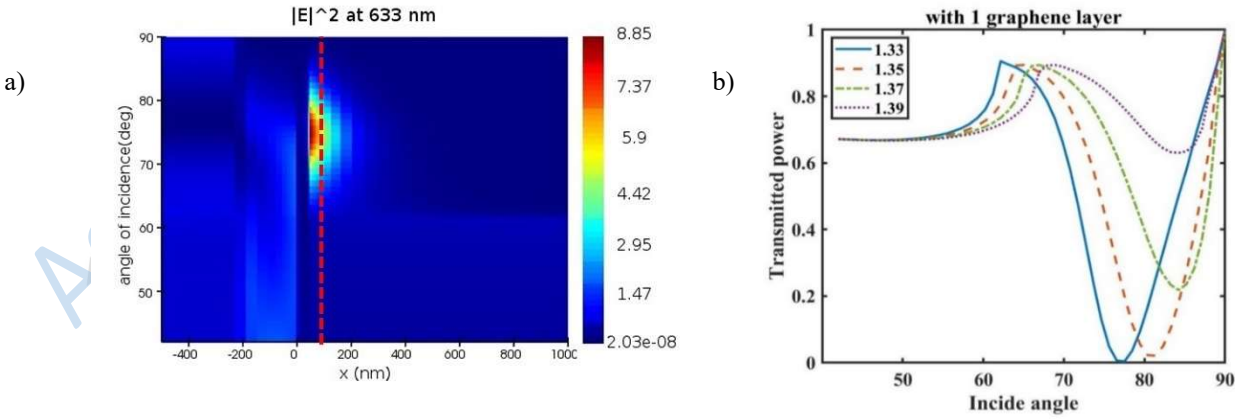

Figure 4. a) Electric field distribution, b) power transmitted through the sensor with a graphene/MoS_2 layer for changes in the input angle for detecting biomaterial with refractive indices of 1.33, 1.35, 1.37 and 1.39**.**

Table 1. Basic parameters of the optical waveguide biosensor with a single layer of graphene and MoS_2.

n_s	θ_{min} (deg)	$\Delta\theta_{0.5}$ (deg)	S (deg/RIU)	Q_f (RIU^{-1})	T_{min}	T_{Max}

1.33	77.37	11.01	-----	-----	0	0.9
1.35	81.23	11.62	193	16.6	0.02	0.89
1.37	84.22	10.59	171.25	16.17	0.22	0.89
1.39	84.29	9.76	115.33	11.81	0.62	0.89

were also indicated in Fig. 4a and Fig. 6a so that the field behavior and penetration characteristics can be clearly observed. The results showed that increasing the number of graphene and MoS_2 layers increases field damping and optical losses, which reduces field localization in the analyte region. As a result, the interaction between the evanescent field and biomolecules becomes weaker, leading to reduced sensitivity and FOM. According to the obtained results, main function parameters of the sensor of the SPR are determined based on the sensitivity, discovery precision and quality factor. Sensitivity of the S is introduced as ratio of the change in incidence angle with minimum transmitted light power or in other words, the SPR angle ($\Delta\theta_{SPR}$) to the change in detection medium refractive index proportional to the alternation in biological material (Δn_a) as equation 2 [58, 59] and its unit is considered as deg/RIU. When DNA is adsorbed onto the sensor surface, the refractive index of the surrounding medium changes. This change alters the resonance condition between the incident light and the surface plasmon, resulting in a shift in the resonance angle. According to the sensor sensitivity relation (Equation 2 [58,59]), the larger the angle shift for a small refractive index change, the more sensitive the sensor becomes. Accordingly, the optimized structure is introduced as the proposed sensor configuration. The detection precision or resolution leans on full-wavelength at the half maximum (FWHM) ($\Delta\theta_{0.5}$), and factor of quality is generated from sensitivity ratio to FWHM (as equation 3 [58,59].

According to the obtained results, the basic parameters of the biosensor with a graphene layer and a MoS_2 layer are compared with each other in Table 1. According to the obtained results, the highest sensitivity for the biomaterial with a refractive index n_s=1.35 is 192deg/RIU. Therefore, it is seen that molecules of the DNA shift angle of SPR to right or to larger values due to their addition to the medium, which alternations of the sensing dielectric refractive index. By introducing DNA as electron-affluent molecules, the number of carriers should change in concentration of the layer of the graphene- MoS_2, causes to a change in diffusion perpetual. So, suggested SPR sensor with extreme sensitivity can be used to identify the DNA hybridization based on SP angle changes. The sensitivity behavior in SPR structures is not always completely linear and may depend on plasmonic coupling conditions, field localization, and the shape of the resonance dip. In the proposed structure, increasing the refractive index of the sensing environment changes the phase matching condition between the waveguide mode and the surface plasmon mode. This can alter the rate of resonance angle shift. It was also observed that with increasing refractive index of the sensing environment, the resonance dip becomes broader and shallower, which can reduce the calculated sensitivity at higher refractive index values. The increase of T_{min} with increasing refractive index indicates that the resonance dip gradually becomes shallower, which may affect the precision of determining the resonance angle and consequently influence the limit of detection. However, in this study, the primary focus has been on sensitivity and FOM.

To investigate effectiveness of sensing characteristics by changes in structural parameters, another waveguide biosensor with three MoS_2/graphene layer pairs has been designed as depicted in Fig. 5. Laser source of light is irradiated into optical waveguide structure. The distribution of the electromagnetic field and the corresponding light passing through the waveguide are calculated for different angles of incidence. The results obtained for biomaterials with different refractive indices

have been depicted in Fig. 6. Increasing the number of graphene/ MoS_2 layers enhances optical absorption and surface plasmon damping in the structure. In Figures 4a and 6a have been shown the electric field distribution $|E|^2$ for structures which containing one pair and three pairs of graphene/ MoS_2 layers at a wavelength of 633 nm. Comparison of these two figures demonstrates that by increasing the number of layers, the intensity and localization of the electromagnetic field in the sensing region significantly decrease. In the structure containing one layer pair, the evanescent field is more strongly confined near the metal/sensing-medium interface and penetrates more effectively into the analyte region. In contrast, in the three-layer structure, part of the field energy is absorbed and dissipated in the additional graphene/ MoS_2 layers, resulting in reduced field amplitude near the sensing medium. As observed in Fig. 6a, the field intensity near the 100 nm region is considerably weaker for the three-layer structure compared to the single-layer structure. This reduction in field localization weakens the coupling between the waveguide mode and the surface plasmon mode, and also reduces the penetration depth of the evanescent field into the sensing medium. Consequently, refractive index variations in the medium have less influence on the resonance condition and resonance angle shift. Furthermore, increasing the number of layers broadens the resonance dip and increases the FWHM, indicating degradation of the plasmonic resonance quality. Therefore, the sensitivity of the structure decreases from about 193 deg/RIU for one-layer pair to about 104 deg/RIU for three-layer pairs.

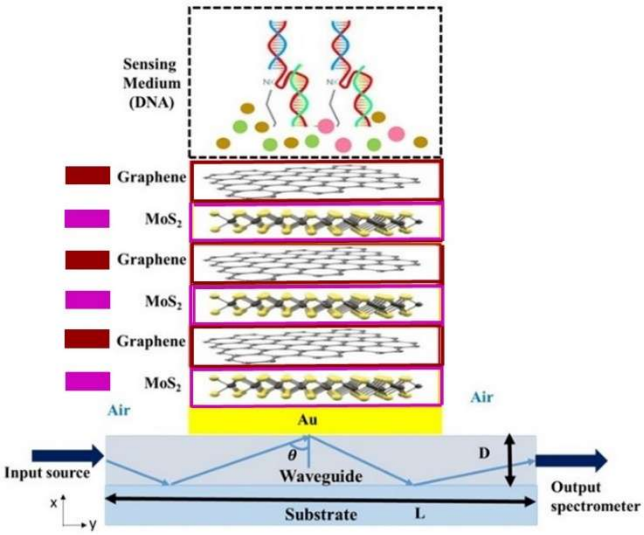

Figure 5. Optical waveguide biosensor structure with three MoS_2/graphene layer pairs.

According to the results obtained, the basic parameters of the biosensor with three pairs of graphene/ MoS_2 layers are compared with each other in Table 2. According to the results obtained,

it can be seen that the minimum angle has shifted towards larger angles compared to the structure with a graphene layer and the MoS_2. The sensitivity and quality factor have also become lower compared to the first structure. The refractive index values of 1.35, 1.37, and 1.39 were considered as effective sensing-medium values after DNA hybridization [58]. These variations represent changes in the optical properties of the medium due to increased DNA molecule concentration and enhanced molecular binding near the sensor surface.

Table 2. Basic parameters of the optical waveguide biosensor with three graphene/ MoS_2 layer pairs.

n_s	θ_{min} (deg)	$\Delta\theta_{0.5}$ (deg)	S (deg/RIU)	Q_f (RIU^{-1})	T_{min}	T_{Max}
1.33	79.58	----	----	----	0.18	0.9
1.35	81.66	14.69	104	7.07	0.34	0.9
1.37	82.39	16.62	70.25	4.22	0.54	0.9
1.39	82.39	11.87	46.83	3.94	0.72	0.9

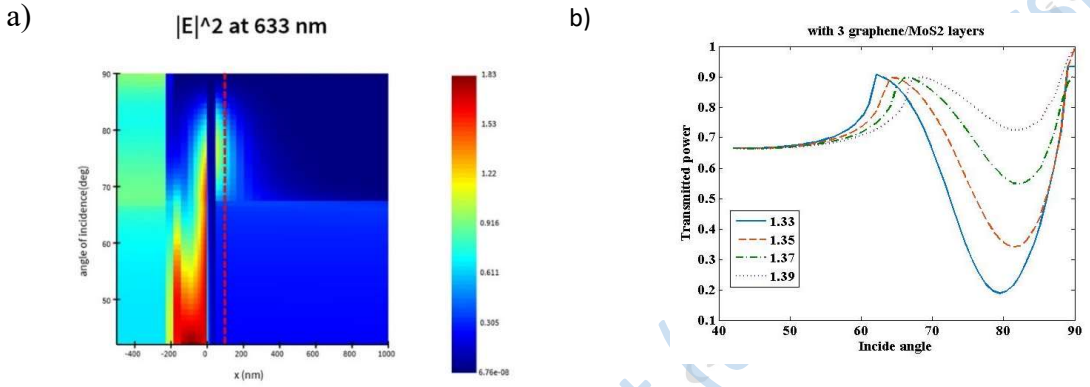

Figure 6. a) Electric field distribution , b)Power transmitted through the sensor with three pairs of graphene/MoS_2 layers for changes in the input angle for detecting biomaterial with refractive indices of 1.33, 1.35, 1.37 and 1.39.

Since the primary objective of this study is to investigate the relative sensor performance against refractive index variations, the effective refractive index approach has been employed, and these values have not been limited to a specific DNA sequence. In addition, increasing the degree of hybridization and biomolecular accumulation on the sensor surface increases the refractive index of the sensing environment, resulting in a resonance angle shift.

In another proposed structure, to investigate the effectiveness of sensing characteristics by changing structural parameters, another waveguide biosensor with one MoS_2 layer and five graphene layers is considered, which has the same total thickness as the previous structure, but all the upper graphene layers have been selected and has a structure as shown in Fig. 7. For the irradiation of a laser light source into the optical waveguide structure, the distribution of the electromagnetic field and the corresponding light passing through the waveguide are calculated by varying different angles of incidence. The results for biomaterials with different refractive indices have been represented in Fig. 8. To investigate the effect of increasing graphene thickness on plasmonic coupling, biological molecule adsorption, and sensor sensitivity, this structure was evaluated. The results showed that increasing the number of graphene layers up to an optimal value improves sensor performance; however, excessive increase in the number of graphene layers leads to higher optical losses, weakening of the plasmonic field, and ultimately a reduction in sensor sensitivity.

The optical properties of graphene depend on the number of layers, and multilayer structures exhibit behavior different from ideal monolayer graphene. In multilayer structures, interlayer interactions and changes in optical conductivity can modify the effective refractive index and plasmonic response of the structure, especially in the visible region where interlayer coupling

becomes more significant. In this study, a constant refractive index value has been used for graphene in order to simplify the FDTD model and focus on investigating the general trend of sensor

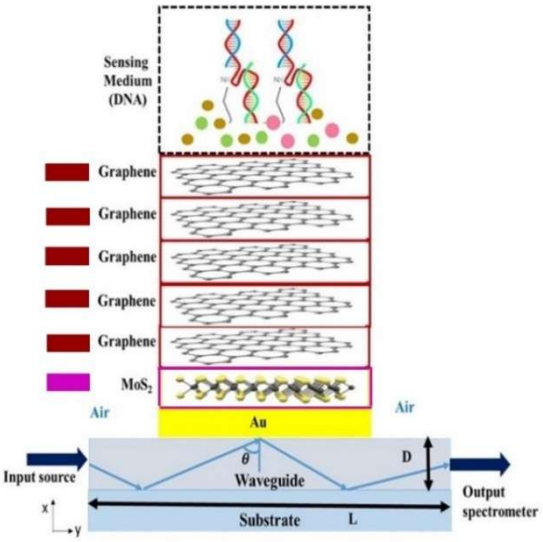

Figure 7. Optical waveguide biosensor structure with one MoS_2 layer and five graphene layers.

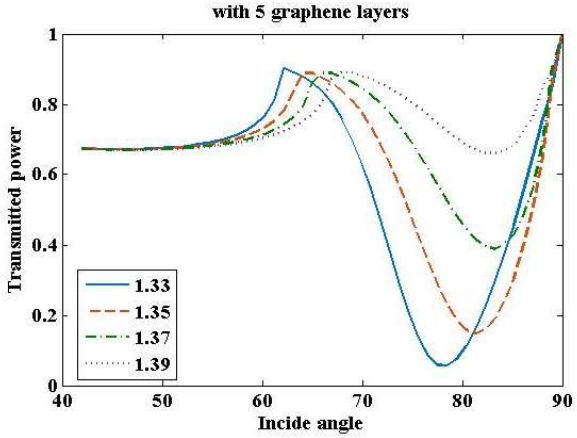

Figure 8. Power transmitted through the sensor with one MoS_2 layer and five graphene layers for changes in the input angle for detecting biomaterial with refractive indices of 1.33, 1.35, 1.37, and 1.39.

performance variations. The main purpose of studying the five-layer structure was not to precisely model the electronic behavior of multilayer graphene, but rather to investigate the effect of increasing the number of layers on plasmonic coupling, optical losses, and sensing performance.

Simulation results demonstrated that increasing the number of graphene layers enhances optical absorption and plasmonic damping. This broadens the resonance dip and reduces evanescent field localization in the sensing region, ultimately decreasing sensitivity and FOM. This behavior is consistent with the expected physical trend in multilayer structures. It should also be noted that the five-layer structure investigated in this paper is physically closer to a few-layer graphitic structure than to ideal monolayer graphene.

According to the obtained results, the basic parameters of the biosensor with three pairs of graphene/MoS2 layers are compared with each other in Table 3. Comparing the results of this structure with the previous structures, it can be seen that the sensitivity and quality factor in this structure are higher than the second structure, but are reduced compared to the first structure. This indicates that having one MoS_2 layer will increase the biosensor performance, while increasing the number of layers will decrease the biosensor performance. For a comparative display of the basic parameters in the three structures, changes in sensitivity have been shown in Fig.9a, and the quality factor with respect to changes in biological substance refractive index has been given in Fig. 9b.

Table 3. Basic parameters of the optical waveguide biosensor with one MoS_2 layer and five graphene layers.

n_s	θ_{min} (deg)	$\Delta\theta_{0.5}$ (deg)	S (deg/RIU)	Q_f (RIU^{-1})	T_{min}	T_{Max}
1.33	77.97	----	---	---	0.05	0.9
1.35	81.17	14.36	160	11.14	0.14	0.89
1.37	83.19	15.21	130.5	8.57	0.38	0.89
1.39	83.29	10.75	88.66	8.28	0.66	0.89

a)

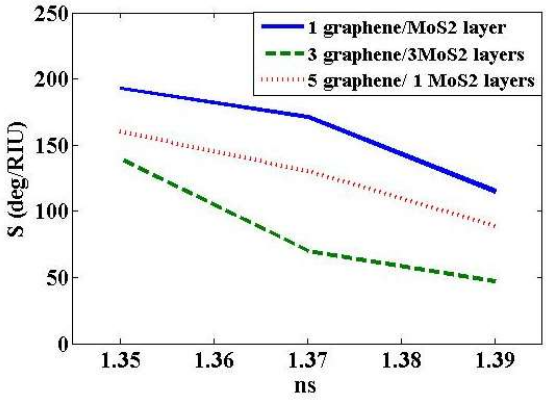

b)

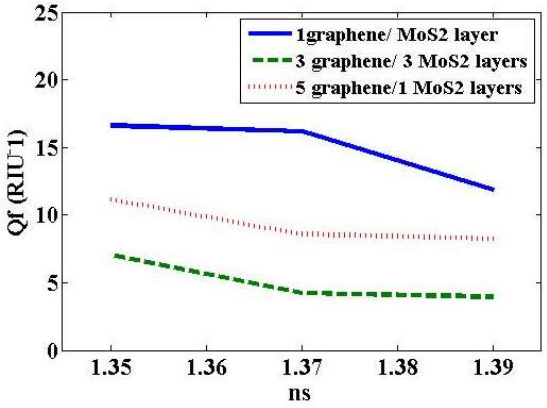

Figure 9. a) Changes in sensitivity for the three introduced structures relative to changes in refractive index, b) quality factor for the three introduced structures relative to changes in refractive index.

Table 4. Comparison of basic parameters of the three proposed structures.

Structure	θ_{min} (deg)	$\Delta\theta_{0.5}$ (deg)	S (deg/RIU)	Q_f (RIU^{-1})	T_{min}	T_{Max}
1graphene/1 MoS_2	81.23	11.62	193	16.6	0.02	0.89
3 graphene/ 3 MoS_2	81.66	14.69	104	7.07	0.34	0.9
5 graphene/ 1 MoS_2	81.17	14.36	160	11.14	0.14	0.89
Au-MoS_2-Graphene-Analyte (PBS) [60]	55.5-66.4	0.4-11.3	80	23.2	-	-
CaF_2-Cu-Ni-BTO-GO [61]	-	-	157.8	17.48	-	-

4. Conclusion

Plasmonic is a large part of the field of nanophotonic that deals with discovering solutions for confining the electromagnetic field in smaller wavelength dimensions. It also has many applications, including chemical and biological sensing, solar cells, and high-resolution imaging, with the exceptional optical properties of metallic nanostructures, including absorption, scattering, and local field enhancement. Plasmonic is based on interaction process between electromagnetic waves and the free electrons in metals or in small metallic nanostructures, and leads to the amplification of the optical near field in subwavelength dimensions. One of the most critical components of nanoplasmonic is the use of metallic nanostructures with unique optical properties. Changing the material, structure, and size of plasmonic nanostructures can affect the increasing the sensitivity in biosensors based on surface plasmons. In this paper, the sensitivity of biosensors of the surface plasmon resonance of 2D materials with waveguide coupling structure has been studied. Although graphene plays an important role in enhancing interaction with biomolecules and improving sensitivity, MoS_2 also has an effective role in the performance of the hybrid structure. Due to its high refractive index and suitable optical absorption properties, MoS_2 improves the confinement of the electromagnetic field near the metal surface. This leads to enhanced plasmonic coupling and increased localization of the evanescent field in the sensing region. In addition, the presence of MoS_2 can strengthen the optical interaction between Au and graphene and improve the SPR response. Therefore, the performance of the proposed structure is not solely due to the presence of graphene, but rather results from the combined effect of graphene and MoS_2.

In addition, the effect of the presence of plasmonic nanostructures and their related parameters on sensitivity of biosensors based on the surface plasmon resonance has been identified and investigated. To achieve this goal, first, various types of biosensor structures based on optical waveguides and simulated biosensors have been introduced, and then the field distribution and power spectrum transmitted through the waveguide sensor with different layers of MoS_2 and graphene have been investigated. In the proposed structure, the simultaneous use of graphene and MoS_2 significantly improves the performance of the SPR sensor. Graphene, due to its high electronic conductivity and high carrier mobility, enhances the concentration of the electromagnetic field near the sensor surface, provides a large specific surface area for better adsorption of DNA and biological molecules, and strengthens the coupling between light and surface plasmons. As a result, the sensor's ability to detect refractive index changes is improved, leading to a sensitivity of about 193 deg/RIU, which demonstrates better performance compared to conventional structures. It should be noted that the results of the proposed model and structure show significant agreement with the findings and simulations of previous studies [58], which indicates the high precision and validity of the proposed model and structure. The proposed biosensor incorporates a combination of MoS_2, graphene, waveguide, and metal layers in a single structure. The purpose of investigating different structures, including multi-bilayer, single-layer, and multilayer configurations, was not only to perform numerical comparisons but also to examine the effect of layer number on the plasmonic behavior and sensor performance. To enhance light absorption, strengthen light–matter interactions, and increase the field interaction

with the structure in the sensing region farther from the waveguide, the number of Graphene/MoS_2 layers was increased. Simulation results showed that although adding more layers can increase light absorption in the structure, it simultaneously leads to higher optical loss and plasmonic damping. As a result, the resonance dip broadens, and the intensity of the evanescent field in the sensing region decreases. This reduction in field confinement weakens the interaction with the analyte and ultimately reduces both the sensitivity and the figure of merit (FOM). The aim of this study was to achieve a balance between these two competing effects. Among all the investigated configurations, the structure consisting of a single graphene layer and a single MoS_2 layer (a single G/ MoS_2 bilayer) provided the optimal balance between plasmonic coupling, field confinement, and optical loss, thereby achieving the best sensing performance. The multilayer structures in the study offer valuable physical insight into the effect of increasing the number of layers on resonance quality and sensor performance, demonstrating that adding more 2D material layers does not necessarily improve the performance of an SPR biosensor. This makes our design more sensitive and easier to integrate than traditional fiber SPR biosensors. Angle determination methods have been used to tune the resonance conditions for the analysis of presented SPR sensor. Designed sensor can detect DNA hybridization with high sensitivity as well as high detection precision and quality factor. At the same time, the proposed sensor is straightforward to manufacture, making it a competitive option for various biosensor applications. Three different biosensor structures with various numbers of layers have been investigated. The basic parameters of sensitivity and quality factor for each of the structures have been studied for different biomaterials. The sensitivity of the proposed sensor depends on the amount of SPR resonance angle shift with respect to changes in the refractive index of the surrounding medium. Simulation results demonstrated that the structure containing one graphene layer and one MoS_2 layer provides the highest sensitivity because the plasmonic field is more strongly confined near the sensor surface and can better detect small refractive index variations caused by the presence of biological molecules. Selectivity refers to the ability of the sensor to distinguish changes caused by specific biomolecules such as DNA. In this structure, selectivity is achieved through the direct dependence of the resonance angle on the refractive index of the sensing medium, such that small changes in DNA concentration or hybridization produce measurable shifts in the transmission spectrum. Reliability of the sensor is related to the stability of the resonance response, the repeatability of the simulation results, and the stable behavior of the structure over different refractive index ranges. The results showed that the proposed structure exhibits a uniform resonance response and predictable variations in the resonance angle, indicating stable and reliable sensor performance [62]. The best results obtained for each of the three proposed structures have been compared in Table .4. The results presented in Table 4 indicate that the best sensor performance corresponds to the structure containing one graphene layer and one MoS_2 layer. This structure provides the highest sensitivity of 193 deg/RIU and the highest FOM value of 16.6 RIU^{-1}, indicating excellent sensor performance in detecting small refractive index variations. In this case, the minimum T_{min} and the narrowest resonance curve were also observed, indicating stronger plasmonic coupling and higher detection accuracy. The results in Table. 4 also show that although increasing the number of graphene and MoS_2 layers enhances optical absorption, it also increases losses and surface plasmon damping, leading to broader resonance dips, increased FWHM, and reduced sensitivity and FOM. Therefore, the

single-layer structure provides the best balance between electromagnetic field confinement, optical losses, and sensor performance. As the comparison of the results shows, the smallest FWHM, highest sensitivity value, highest excellence factor, and also the lowest transmission intensity value is related to the structure with a single graphene layer. In the single-layer structure, optical absorption losses and plasmon damping are lower, and the coupling between light and surface plasmons occurs with higher quality. As a result, the resonance curve becomes narrower and the FWHM decreases. However, in multilayer structures, due to increased losses and damping, the resonance curve broadens and the detection accuracy decreases. Therefore, it provides the most appropriate performance among the proposed structures. The physical analysis performed shows that in the single-layer structure, the electromagnetic field is more strongly confined near the sensor surface and there is greater overlap between the evanescent field and biomolecules (Figures 4a and 6a). This enhances the interaction between light and matter, leading to increased sensitivity. In multilayer structures, the increased effective thickness of graphene and MoS_2 layers leads to higher absorption loss and plasmon damping. These losses reduce the penetration depth of the field into the sensing medium, broaden the resonance dip, and reduce sensitivity and detection precision. To evaluate the performance of the proposed structure, the results of this study were compared with several recent investigations on SPR sensors based on two-dimensional materials, as presented in Table 4. As observed, the proposed structure demonstrates acceptable performance in terms of sensitivity and figure of merit compared to Au– MoS_2–graphene sensors as well as CaF_2-Cu-Ni-BTO-GO structures. This comparison highlights the capability of the proposed structure to improve the plasmonic response and enhance sensor precision [60-62].

Although the sensitivity of the proposed structure is appropriate, the presence of two-dimensional layers and the optical losses associated with the hybrid structure has been led to a broader resonance dip and increased FWHM, which ultimately reduce the FOM. In addition, multilayer structures can increase plasmonic damping and reduce the resonance quality.

Availability of data and materials

The authors declare that the data supporting the findings of this study are available within the paper.

Conflict of interests

The authors assert that they do not have any identifiable conflicting financial interests or personal relationships that might be perceived

to influence the work presented in this paper.

Funding

No funding was obtained for this study.

References

[1] Alwan, A.M., A.A. Yousif, and L.A. Wali, *The growth of the silver nanoparticles on the mesoporous silicon and macroporous silicon: a comparative study*. Indian Journal of Pure & Applied Physics, 2017. 55(11): p. 813–820. Available at: https://nopr.niscpr.res.in/handle/123456789/43261 .

[2] Choi, S.H., Y.L. Kim, and K.M. Byun, Graphene-on-silver substrates for sensitive surface plasmon resonance imaging biosensors. Optics express, 2011. 19(2): p. 458466.https://doi.org/10.1364/oe.19.000458

[3] Halterman, K. and M. Alidoust, Waveguide modes in Weyl semimetals with tilted dirac cones. Optics Express, 2019. 27(25): p. 3616436182.https://doi.org/10.1364/oe.27.036164.

[4] Ghasemzadeh N, Rahatabad FN, Haghipour S, Miandoab SA, Maghooli K. Controlling pathological activity of Parkinson basal ganglia based on excitation and inhibition optogenetic models and monophasic and biphasic electrical stimulations. J Biosci. 2023; 48:40. PMID: 37846022.http://dx.doi.org 10.1007/s12038-023-00359-x.

[5] Miandoab SA, Ghasemzadeh N. Modeling the neurodegenerative Parkinson's disease treatment with high effectiveness of beta-band neural activity using the optogenetic-electrical hybrid stimulation. Biomedical Signal Processing and Control. 2025 Dec 1;110:107999.https://doi.org/10.1016/j.bspc.2025.107999.

[6] Faraji, H., S. Haji-Nasiri, and S.A. Miandoab, Correction: Engineered Graphene-Integrated 3D curved hyperbolic metamaterial nanolenses for advanced multiselective nanophotonic biosensing. Optical and Quantum Electronics, 2025. 57(11): p. 608. https://doi.org/10.1007/s11082-025-08533-1.

[7] Faraji H, Haji-Nasiri S, Andalibi Miandoab S. Plasmonic Mid-infrared Biosensor with High Sensitivity Using Multilayer Graphene/Al2O3 Cylindrical Hyperbolic Metamaterials. Sensing and Imaging. 2026 Feb 19;27(1):34. https://doi.org/10.1007/s11220-026-00730-w.

[8] Parcham, E. and S.A. Miandoab**,** *Introducing nanostructure patterns for performance enhancement in PbS colloidal quantum dot solar cel*ls. International Journal of Nano Dimension, 2020. 11(1). Available at: https://oiccpress.com/ijnd/article/view/4254.

[9] Bozhevolnyi, S.I., et al., Channel plasmon subwavelength waveguide components including interferometers and ring resonators. Nature, 2006. 440(7083): p. 508–511.https://doi.org/10.1038/nature04594.

[10] Ouyang, Q., et al., Sensitivity enhancement of transition metal dichalcogenides/silicon nanostructure-based surface plasmon resonance biosensor. Scientific reports, 2016. 6(1): p. 28190.https://doi.org/10.1038/srep28190.

[11] Wali, L.A., et al., Excellent fabrication of Pd-Ag NPs/PSi photocatalyst based on bimetallic nanoparticles for improving methylene blue photocatalytic degradation. Optik, 2019. 179: p. 708–717. https://doi.org/10.1016/j.ijleo.2018.11.011.

[12] Xiao, S., et al., Tunable anisotropic absorption in hyperbolic metamaterials based on black phosphorous/dielectric multilayer structures. Journal of Lightwave Technology, 2019. 37(13): p. 3290–3297.
https://doi.org/10.1109/jlt.2019.2914183 .

[13] Zhang, S., et a***l.,*** *Chiral surface plasmon polaritons on metallic nanowi*r***e***s.* Physical Review Letters, 2011. 107(9): p. 096801. DOI: 10.1103/PhysRevLett.107.096801**.**

[14] Cen, C., et al., A tunable plasmonic refractive index sensor with nanoring-strip graphene arrays. Sensors, 2018. 18(12): p. 4489.https://doi.org/10.3390/s18124489 .

[15] Liang, C., et al., Dual-band infrared perfect absorber based on a Ag-dielectric-Ag multilayer films with nanoring grooves arrays. Plasmonics, 2020. 15(1): p. 93–100.https://doi.org/10.1007/s11468-019-01018-4.

[16] Wang, X., et *al., Tunable terahertz/infrared coherent perfect absorption in a monolayer black phos*phorus. Optics Express, 2018. 26(5): p. 5488–5496. DOI: 10.1364/OE.26.005488.

[17] Ma, Y., et al., A terahertz polarization insensitive dual band metamaterial absorber. Optics letters, 2011. 36(6): p. 945–947.https://doi.org/10.1364/ol.36.000945 .

[18] Yao, G., et al., Dual-band tunable perfect metamaterial absorber in the THz range. Optics express, 2016. 24(2): p. 1518–1527.https://doi.org/10.1364/oe.24.001518 .

[19] Ji, S., et al., Design of a polarization-insensitive triple-band metamaterial absorber. Optics Communications, 2019. 432: p. 65–70.https://doi.org/10.1016/j.optcom.2018.09.040.

[20] Zhang, Y., et al., A graphene based tunable terahertz sensor with double Fano resonances. Nanoscale, 2015. 7(29): p. 12682–12688.https://doi.org/10.1039/c5nr03044g .

[21] Andryieuski, A. and A.V. Lavrinenko, Graphene metamaterials based tunable terahertz absorber: effective surface conductivity approach. Optics express, 2013. 21(7): p. 9144–9155. https://doi.org/10.1364/oe.21.009144 .

[22] Bibikova, O., Haas, J., López-Lorente, A. I., Popov, A., Kinnunen, M., Meglinski, I., & Mizaikoff, B. (2017). *Towards enhanced optical sensor performance: SEIRA and SERS with plasmonic nanostars.* Analyst, 142(6), 951–958. https://doi.org/10.1039/C6AN02596J.

[23] Mejia-Salazar, J.R., et al., New trends in plasmonic (bio) sensing. Anais da Academia Brasileira de Ciências, 2018. 90: p. 779–801.https://doi.org/10.1590/0001376520182017057l.

[24] Lai, W., K. Wen, J. Lin, Z. Guo, Q. Hu, and Y. *Fang, Plasmonic filter and sensor based on a subwavelength end-coupled hexagonal r*esonator. Applied Optics, 2018. 57(22): p. 6369–6374. DOI: 10.1364/AO.57.006369.

[25] Li, H., J. Niu, and G. Wang, Dual-band, polarization-insensitive metamaterial perfect absorber based on monolayer graphene in the mid-infrared range. Results in Physics, 2019. 13: p. 102313. https://doi.org/10.1016/j.rinp.2019.102313

[26] Tsuchikawa, K., et al., Characterization of a Weyl semimetal using a unique feature of surface plasmon polaritons. Physical Review B, 2020. 102(3): p. 035443.https://doi.org/10.1103/physrevb.102.035443.

[27] Ebadi SM, Örtegren J, Bayati MS, Ram SB. A multipurpose and highly-compact plasmonic filter based on metal-insulator-metal waveguides. IEEE Photonics Journal. 2020 Feb 19;12(3):1-9. https://doi.org/10.1109/jphot.2020.2974959.

[28] Wen, C., et al., Enhanced molecular infrared spectroscopy employing bilayer graphene acoustic plasmon resonator. Biosensors, 2021. 11(11): p. 431.https://doi.org/10.3390/bios11110431

[29] Patel, S.K., *et al., Tunable infrared metamaterial-based biosensor for detection of hemoglobin and urine using phase change* material. Scientific Reports, 2021. 11(1): p. 7101. DOI: 10.1038/s41598-021-86583-5.

[30] Bensalah, H., Hocini, A., Bahri, H. *et al.* A plasmonic refractive index sensor with high sensitivity and its application for temperature and detection of biomolecules. *J Opt* 52, 1035–1046 (2023). https://doi.org/10.1007/s12596-022-00922-z.

[31] Miandoab, S.A. and S.S. Hars, Design and simulation of concentrator plasmonic nanostructure optical antenna to improve the performance of Li-Fi communication technology. International Journal of Nano Dimension, 2025. 16(3 (July 2025)). https://dx.doi.org/10.57647/j.ijnd.2025.1603.21.

[32] Shakya AK, Ramola A, Balal N, Bergman A. Evolution of Photonic Crystal Fiber Based Smart Sensors with Emphasis on Biomedical Applications: A Review. IEEE Sensors Journal. 2026 Jan 12. DOI:10.1109/JSEN.2026.3650816.

[33] Ramola A., Shakya A.K., Balal N., Berg*man A. Theoretical Investigation of Early Cancer Biomarker Sensing Using a PMMA–Gold Hybrid Quasi-D-Shaped Photonic-Crystal-Fiber-Based Surface Plasmon Resonance Bi*osensor. Micromachines, 2026, 17(1), 68. https://doi.org/10.3390/mi17010068.

[34] Ramola A., Shakya A.K., Droby A., Berg*man A. Numerical Study of a Novel Kagome-Inspired Photonic Crystal Fiber-Based Surface Plasmon Resonance Biosensor for Detection of Blood Components and Analytical* Targets. Biosensors, 2025, 15(8), 539. https://doi.org/10.3390/bios15080539

[35] Ramola A., Shakya A.K., Kumar V., Berg*man A. Recent Advances in Photonic Crystal Fiber-Based SPR Biosensors: Design Strategies, Plasmonic Materials, and Appli*cations. Micromachines, 2025, 16(7), 747. https://doi.org/10.3390/mi16070747

[36] Ramola A., Shakya A.K., Berg*man A. Finite Element Method-Based Modeling of a Novel Square Photonic Crystal Fiber Surface Plasmon Resonance Sensor with a Au–TiO₂ Interface and the Relevance of Artificial Intelligence Techniques in Sensor Optimi*zation. Photonics, 2025, 12(6), 565. https://doi.org/10.3390/photonics12060565.

[37] Ramola A, Shakya AK, Bergman A. Comprehensive analysis of advancement in optical biosensing techniques for early detection of cancerous cells. Biosensors. 2025 May5;15(5):292..https://doi.org/10.3390/bios15050292.

[38] Shakya A.K., *Singh S. Development of a Generalized Fourier Transform Model for Distinct Household Oil Samples by Performing Spectroscopy* Analysis. Results in Optics, 2023, 10, 100355. https://doi.org/10.1016/j.rio.2023.100355.

[39] Nematpour A, Nikoufard M. Plasmonic thin film InP/graphene-based Schottky-junction solar cell using nanorods. Journal of advanced research. 2018 Mar 1;10:15-20. 10.1016/j.jare.2018.01.008.https://doi.org/10.1016/j.jare.2018.01.008

[40] Mahdian MA, Nikoufard M, Soleimannezhad F. Effect of etching depth on the performance of InP-based hybrid plasmonic waveguides. AEU-International Journal of Electronics and Communications. 2020 Nov 1;126:153403.10.1016/j.aeue.2020.153403.https://doi.org/10.1016/j.aeue.2020.153403.

[41] Soleimannezhad F, Nikoufard M, Mahdian MA. Low-loss indium phosphide-based hybrid plasmonic waveguide. Microwave and Optical Technology Letters. 2021 Sep;63(9):2242-51.10.1002/mop.32488.https://doi.org/10.1002/mop.32488.

[42] Nikoufard M, Kazemi Alamouti M, Adel A. Ultra-compact photonic crystal based water temperature sensor. Photonic Sensors. 2016 Sep;6(3):274-8.10.1007/s13320-016-0321-0. https://doi.org/10.1007/s13320-016-0321-0 .

[43] Nematpour A, Nikoufard M, Mehragha R. Design and optimization of the plasmonic graphene/InP thin-film solar-cell structure. Laser Physics. 2018 Jun 1;28(6):066202.10.1088/1555611/aab462.https://doi.org/10.1088/1555-6611/aab462.

[44] Dalvand H, Nikoufard M, Zangeneh HR. Graphene-based modulator using GST-phase change material on semi-ellipsoid slot waveguide configuration: H Dalvand et al. Indian Journal of Physics. 2025 Feb;99(2):357 66.10.1007/s12648-024-03308-y. https://doi.org/10.1007/s12648-024-03308-y.

[45] Nikoufard M, Alamouti MK, Pourgholi S. Multimode interference power-splitter using InP-based deeply etched hybrid plasmonic waveguide. IEEE Transactions on Nanotechnology. 2017 Mar 28;16(3):477 83.10.1109/TNANO.2017.2688397. https://doi.org/10.1109/tnano.2017.2688397.

[46] Nikoufard M, Nourmohammadi A, Esmaeili S. Hybrid plasmonic nanoantenna with the capability of monolithic integration with laser and photodetector on InP substrate. IEEE Transactions on Antennas and Propagation. 2017 Oct 30;66(1):3-8.10.1109/TAP.2017.2767623.https://doi.org/10.1109/tap.2017.2767623

[47] Yu, P., et al., Metamaterial perfect absorber with unabated size-independent absorption. Optics Express, 2018. 26(16): p. 20471–20480.https://doi.org/10.1364/oe.26.020471

[48] Pan, W., et al., A broadband terahertz metamaterial absorber based on two circular split rings. IEEE Journal of Quantum Electronics, 2016. 53(1): p. 1–6.https://doi.org/10.1109/jqe.2016.2643279.

[49] Khodadad H, Hatamjafari F, Pourshamsian K, Sadeghi B. Microwave-assisted synthesis of novel pyrazole derivatives and their biological evaluation as anti-bacterial agents. Combinatorial Chemistry & High Throughput Screening. 2021 Jun 1;24(5):695-700. https://doi.org/10.2174/1386207323666201019152206.

[50] Pourjafari M, Ghane M, Kaboosi H, Sadeghi B, Rezaei A. Antibacterial properties of Ag–Cu alloy nanoparticles against multidrug-resistant Pseudomonas aeruginosa through inhibition of quorum sensing pathway and virulence-related genes. Journal of Biomedical Nanotechnology. 2022 Apr 1;18(4):1196-204. https://doi.org/10.1166/jbn.2022.3331.

[51] Azari B, Pourahmad A, Sadeghi B, Mokhtary M. Green synthesis of SiO2 from Equisetnm arvense plant for synthesis of SiO2/ZIF-8 MOF nanocomposite as photocatalyst. Journal of Coordination Chemistry. 2023 Jan 17;76(2):219-31. https://doi.org/10.1080/00958972.2023.2166408

[52] Sadeghi B, Vahdati RA. Comparison and SEM-characterization of novel solvents of DNA/carbon nanotube. Applied surface science. 2012 Jan 15;258(7):3086-8. https://doi.org/10.1016/j.apsusc.2011.11.042.

[53] Sohrabnezhad S, Pourahmad A, Sadjadi MS, Sadeghi B. Nickel cobalt sulfide nanoparticles grown on AlMCM-41 molecular sieve. Physica E: Low-dimensional Systems and Nanostructures. 2008 Jan 1;40(3):684-8. https://doi.org/10.1016/j.physe.2007.09.081.

[54] Wang, L. et al., Recent progress in the assembly of nanodevices and van der Waals heterostructures by deterministic placement of 2D materials, Chemical Society Reviews, 2017. https://pubs.rsc.org/en/content/articlehtml/2017/cs/c7cs00556c

[55] Kinoshita, K. et al., Dry release transfer of graphene and few-layer h-BN using polypropylene carbonate, arXiv, 2019. https://arxiv.org/abs/1904.12170

[56] Castellanos-Gomez, A. et al., Van der Waals heterostructures and their assembly techniques, Nature Reviews Methods Primers, 2022.https://www.nature.com/articles/s43586-022-00139-1.pdf

[57] Wang, L. et al., Advances in deterministic transfer methods for 2D materials and van der Waals heterostructures, Nano-Micro Letters, 2019.https://link.springer.com/article/10.1007/s40820-019-0245-5

[58] Rahman, M.S., K.A. Rikta, and M. Anower, Numerical Analysis of MoS_2-Graphene Hybrid Structure Based Planar Waveguide Surface Plasmon Resonance Biosensor for Sensing DNA Hybridization. Sensor Letters, 2017. 15(10): p. 868–875.https://doi.org/10.1166/sl.2017.3886

[59] Chen S, Lin C. Figure of merit analysis of graphene based surface plasmon resonance biosensor for visible and near infrared. Optics Communications. 2019 Mar 15;435:102-7. https://doi.org/10.1016/j.optcom.2018.11.031 .

[60] Bahmani E, Kaatuzian H, Shafagh SG. High-performance Au– MoS_2–graphene multilayer SPR biosensor with superior sensitivity and precision. Scientific Reports. 2026 Feb 12. https://doi.org/10.1038/s41598-026-39993-4.

[61] Runthala R, Venkatesh VK, Gupta D, Arora P. Simulation-Driven Design of a Multilayer Plasmonic Sensor Using Cu-Ni and $BaTiO_2$ for Waterborne Pathogen Detection. In2025 IEEE 20th Nanotechnology Materials and Devices Conference (NMDC) 2025 Oct 9 (pp. 259-264). IEEE. https://doi.org/10.1109/nmdc64551.2025.11233969.

[62] Hocini A, Ben Salah H, Temmar MN. Ultra-high-sensitive sensor based on a metal–insulator–metal waveguide coupled with cross cavity. Journal of Computational Electronics. 2021 Jun;20(3):1354-62. https://doi.org/10.1007/s10825-021-01706-7.